

AD \_\_\_\_\_

Award Number: DAMD17-00-1-0343

TITLE: Organic Polymer Light Emitting Display for Digital  
Mammography

PRINCIPAL INVESTIGATOR: Doctor Joohan Kimis

CONTRACTING ORGANIZATION: The University of Michigan  
Ann Arbor, Michigan 48109-1274

REPORT DATE: March 2003

TYPE OF REPORT: Annual Summary

PREPARED FOR: U.S. Army Medical Research and Materiel Command  
Fort Detrick, Maryland 21702-5012

DISTRIBUTION STATEMENT: Approved for Public Release;  
Distribution Unlimited

The views, opinions and/or findings contained in this report are those of the author(s) and should not be construed as an official Department of the Army position, policy or decision unless so designated by other documentation.

# REPORT DOCUMENTATION PAGE

Form Approved  
OMB No. 074-0188

Public reporting burden for this collection of information is estimated to average 1 hour per response, including the time for reviewing instructions, searching existing data sources, gathering and maintaining the data needed, and completing and reviewing this collection of information. Send comments regarding this burden estimate or any other aspect of this collection of information, including suggestions for reducing this burden to Washington Headquarters Services, Directorate for Information Operations and Reports, 1215 Jefferson Davis Highway, Suite 1204, Arlington, VA 22202-4302, and to the Office of Management and Budget, Paperwork Reduction Project (0704-0188), Washington, DC 20503

<b>1. AGENCY USE ONLY</b> (Leave blank)		<b>2. REPORT DATE</b> March 2003	<b>3. REPORT TYPE AND DATES COVERED</b> Annual Summary (1 Mar 2000 - 29 Feb 2003)	
<b>4. TITLE AND SUBTITLE</b> Organic Polymer Light Emitting Display for Digital Mammography			<b>5. FUNDING NUMBERS</b> DAMD17-00-1-0343	
<b>6. AUTHOR(S)</b> Doctor Joohan Kimis				
<b>7. PERFORMING ORGANIZATION NAME(S) AND ADDRESS(ES)</b> The University of Michigan Ann Arbor, Michigan 48109-1274  <i>E-Mail:</i>			<b>8. PERFORMING ORGANIZATION REPORT NUMBER</b>	
<b>9. SPONSORING / MONITORING AGENCY NAME(S) AND ADDRESS(ES)</b> U.S. Army Medical Research and Materiel Command Fort Detrick, Maryland 21702-5012			<b>10. SPONSORING / MONITORING AGENCY REPORT NUMBER</b>	
<b>11. SUPPLEMENTARY NOTES</b> Original contains color plates: All DTIC reproductions will be in black and white.				
<b>12a. DISTRIBUTION / AVAILABILITY STATEMENT</b> Approved for Public Release; Distribution Unlimited			<b>12b. DISTRIBUTION CODE</b>	
<b>13. ABSTRACT (Maximum 200 Words)</b> We report on active-matrix organic polymer light-emitting displays (AM-OLEDs) based on a three hydrogenated amorphous silicon (a-Si:H) thin-film transistor (TFT) pixel electrode circuit that supplies a continuous output current to organic polymer light-emitting devices (OLEDs). The output current level drifts induced by either process variations or devices aging can be reduced in this design by adjusting the driver TFT operating point with the active resistor. Our first green light-emitting engineering prototype had a brightness of 120 cd/m <sup>2</sup> and fill factor of about 45%.				
<b>14. SUBJECT TERMS</b> Flat panel display, a-Si:H TFTs, AM-OLEDs, OLEDs, organic light-emitting devices			<b>15. NUMBER OF PAGES</b> 25	
			<b>16. PRICE CODE</b>	
<b>17. SECURITY CLASSIFICATION OF REPORT</b> Unclassified	<b>18. SECURITY CLASSIFICATION OF THIS PAGE</b> Unclassified	<b>19. SECURITY CLASSIFICATION OF ABSTRACT</b> Unclassified	<b>20. LIMITATION OF ABSTRACT</b> Unlimited	

# Contents

1.	Cover page	1
2.	SF298	2
3.	Introduction	3
4.	Body	5
	4.1 Pixel electrode circuit construction and schematics	5
	4.2 Pixel electrode circuit design	7
	4.3 Pixel electrode driving scheme	9
	4.4 Pixel electrode circuit simulation	10
	4.5 AM-OLED operation	14
	4.6 AM-OLED pixel electrode circuits fabrication	15
	4.7 AM-OLED pixel electrode circuit performance	18
	4.8 AM-OLED opto-electronic properties	19
	References	22
5.	Key research accomplishments	24
6.	Reportable outcomes	24
7.	Appendix	

### 3. INTRODUCTION

In 1990, the flat panel display world was surprised when a group at Cambridge University (U.K.) demonstrated the first light-emitting plastic device – the organic polymer light-emitting diode (OLED) had been born. Several research and industrial groups, including our group at the University of Michigan, soon recognized the potential of this technology to produce ultra-thin, flat, low-power, very bright, wide viewing angle, potential low cost, and lightweight displays with CRT-like performance that could challenge the active-matrix liquid-crystal displays (AM-LCDs) – the flat panel display industry's benchmark. The OLED-based display addressing can be achieved by using either passive or active-matrix arrays. However, passive-matrix-addressed display performances are limited in term of luminance because the pixels are in the ON-state only during a small portion of the addressing time. Considering a pixel luminance of about  $100 \text{ cd/m}^2$ , a duty cycle of 50% and assuming that the pixel aperture ratio is 100%, we can show that the maximum number of lines in such a display is about 35. Such a low value is not compatible with the size and resolution required for medical imaging displays, and active-matrix addressing is therefore necessary. An additional advantage of the active-matrix organic light-emitting displays (AM-OLEDs) is that the voltage across each pixel can be set within the thin film transistor (TFT) active-matrix array alone, with the OLED cathode set at a fixed voltage. Over the last several years there have been many efforts in different laboratories to develop various configurations of the AM-OLEDs since different types of the OLEDs [1,2,3,4] have been introduced [5,6,7]. Also over the time the number of TFTs associated with the pixel electrode has increased from two to four TFTs. Initially the AM-OLEDs with two TFTs have been developed by directly adapting the pixel electrode circuit design developed for the active-matrix liquid-crystal displays (AM-LCDs) [5,6]. One TFT is used as switching element, while the other controls the display brightness, and the storage capacitor serves as the charge reservoir to maintain the constant current flow during the pixel OFF-period. However, threshold voltage variations of the drive TFT, resulting from manufacturing variations or long-term display operation, could lead to a severe pixel electrode gray-level errors that will produce a luminance variation across the display. Hence, these circuits could not meet the requirements of the AM-OLEDs for medical imaging. More specifically these circuits could not compensate for the threshold voltage shift of TFTs and the turn-on voltage shift of the OLED that can be introduced during the display operation. By adding two more TFTs, advanced AM-OLEDs with four TFTs have been developed [7]. Although the four TFT pixel electrode circuits featured constant current driving and voltage shift compensation, metal interconnections and four TFTs consumed large pixel area. This will reduce the pixel aperture ratio and can prevent the development of the high-resolution displays. Also so far all AM-OLEDs are based on poly-crystalline silicon (poly-Si) TFT technology. It is believed that a low current capacity of a-Si:H TFTs [8,9] in comparison with the poly-Si TFTs is inadequate for AM-OLEDs. However, some recent initial results obtained in our laboratory [10,11,12] have proven that a combination of high-efficiency OLED and high-performance a-Si:H TFT can be sufficient for AM-OLEDs. We believe that combining OLEDs with a-Si:H TFTs technology will have tremendous advantages over the AM-LCDs resulting in a low cost display that can be produced over a large area on flexible plastic substrates.

The electronic display of mammographic images remains today an important technological barrier for the deployment of fully digital mammography systems. Extremely high-resolution

displays are required to detect and characterize small lesions in mammograms. In addition, good display contrast resolution is needed to achieve high medical diagnostic performance when subtle details are present in low-luminance image regions [13,14]. Among the different technologies that can promise unhurt display of mammographic images are thin emissive devices such as AM-OLEDs. This type of flat panel display can provide quasi-Lambertian emission over a large area with acceptable resolution, while performing even better than film in some other performance areas. Table 1 summarizes the state-of-the-art for CRT and AM-LCD displays, and compares their performance with mammographic film quality and with the achievable quality of the AM-OLEDs.

Table 1. Display specifications of current medical imaging display devices.

SPECIFICATION	MAMMOGRAPHIC FILM	CRT <sup>(1)</sup>	AM-LCD <sup>(2)</sup>	AM-OLED <sup>(3)</sup>
Size (cm)	24 × 30	30 × 36	20 × 20	NA
Pixel array size	4000 × 5000	2500 × 2000	7860 × 2048	7860 × 2048
Pixel size (μm)	50	120	50	50
Max luminance (nit)	3000	300	230	> 2000
Min luminance (nit)	1	2	1	< 1
Gray-scale Emission	≥ 920	~ 500	NA	NA
Color	Lambertian Monochrome	Lambertian Monochrome	Non-Lambertian Color/mono	Lambertian Monochrome
Veiling glare ratio <sup>(a)</sup>	> 1000	140	NA	> 1000
Diffuse reflect. (sr <sup>-1</sup> )	~ 0.02	0.03	NA	0.005
Specular reflect. Viewing angle (V)	~ 0.02 full	0.005 full	0.005 < ± 80 <sup>(b)</sup>	0.005 full
Viewing angle (H)	full	full	< ± 80 <sup>(b)</sup>	full

<sup>(1)</sup> Specifications for high-performance CRTs manufactured by several companies.

<sup>(2)</sup> Based on best devices.

<sup>(3)</sup> Based on computational model predictions.

<sup>(a)</sup> Based on the dark spot measurement method with a 1-cm spot.

<sup>(b)</sup> Based on isocontrast curves of 10:1 full-field contrast ratio.

In general, because the AM-OLEDs are based on all solid-state physics (the light emission is generated through the recombination process of carriers injected from cathode and anode electrodes), we expect that this type of display to have several attractive features:

- **Resolution and brightness:** Resolution of 50 μm can be easily achieved in AM-OLED without any loss of display contrast. The brightness of 2000 cd/m<sup>2</sup> can be easily realized also for a given color.

- **Contrast ratio:** The ability to generate high brightness and maintain a controlled low value for the minimum luminance determines a high large-area and small-spot contrast ratio and low veiling glare.
- **Viewing angle:** No dependency of the gray-scale or contrast on the viewing direction is expected, since the AM-OLEDs have a quasi-Lambertian emission distribution of generated light.
- **Gray-scale:** The luminance of the OLED is directly proportional to current injection and therefore can be controlled with precision, since in the AM-OLEDs the relation between the signal and the pixel luminance is linear.
- **Low and high temperature operation:** In the temperature range between  $-30$  and  $+85$   $^{\circ}\text{C}$ , the conducting polymers and OLEDs remain stable.
- **Flexibility, reduced weight and improved ruggedness:** The plastic substrates will allow producing a compact, lightweight (1/6 of the glass substrate), robust (shockproof), and cost effective (roll-to-roll process) flat panel display technology.

The most important factors from the above list to be considered for the application of the AM-OLED to digital mammography are resolution and brightness, along with wide viewing angle, high contrast ratio, large gray-scale, and practical lifetime. Today we can notice that OLED lifetime has improved by factors of 10 every year, and are currently in excess of 10,000 hours for some colors.

The objective of this research was to develop a plastic display device that could replace mammographic film with improved display quality in comparison with the CRT.

## 4. BODY

### 4.1 PIXEL ELECTRODE CIRCUIT CONSTRUCTION AND SCHEMATICS

In the AM-LCDs, each pixel is composed of one switching device (a-Si:H TFT), LC capacitor, and storage capacitor, Figure 1. The main issue in this type of display is to charge LC capacitor within given scan time (typically 30  $\mu\text{sec}$  and 20  $\mu\text{sec}$  for VGA and XGA AM-LCDs, respectively), and to retain the charge level until the next charging time. Each image pixel data is converted to a charge and stored in the LC capacitor through a-Si:H TFT. The image data have to be retained for one frame time (60 Hz).

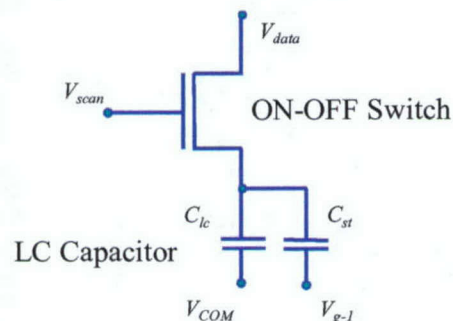


Figure 1. Typical equivalent circuit schematic of AM-LCD is shown.

The AM-OLEDs, however, demand some extra functionality in active pixel electrode circuitry in comparison with the AM-LCDs. These are active addressing circuit, constant current driving circuit, current-compensation circuit, and OLED, Figure 2 (a). The active addressing circuit consists of a switching TFT and a storage capacitor performing the identical function to AM-LCD counterpart. The image data are converted to charges and stored in the storage capacitors through switching TFTs associated with each pixel. The constant current driving pixel electrode circuit is a large-sized high-capacity TFT supplying constant current needed for OLED operation. Unlike LC capacitor, OLED keeps dissipating a certain amount of constant current during the light emitting process. In Figure 2, the current-compensation circuit is an active resistor. The active resistor attached to the constant current driving TFT and the OLED senses the current level flowing through the OLED during the pixel operation, and keeps it constant when current shift is induced by threshold voltage shift in the constant current driving TFT or by turn-on voltage shift in the OLED, Figure 2 (b).

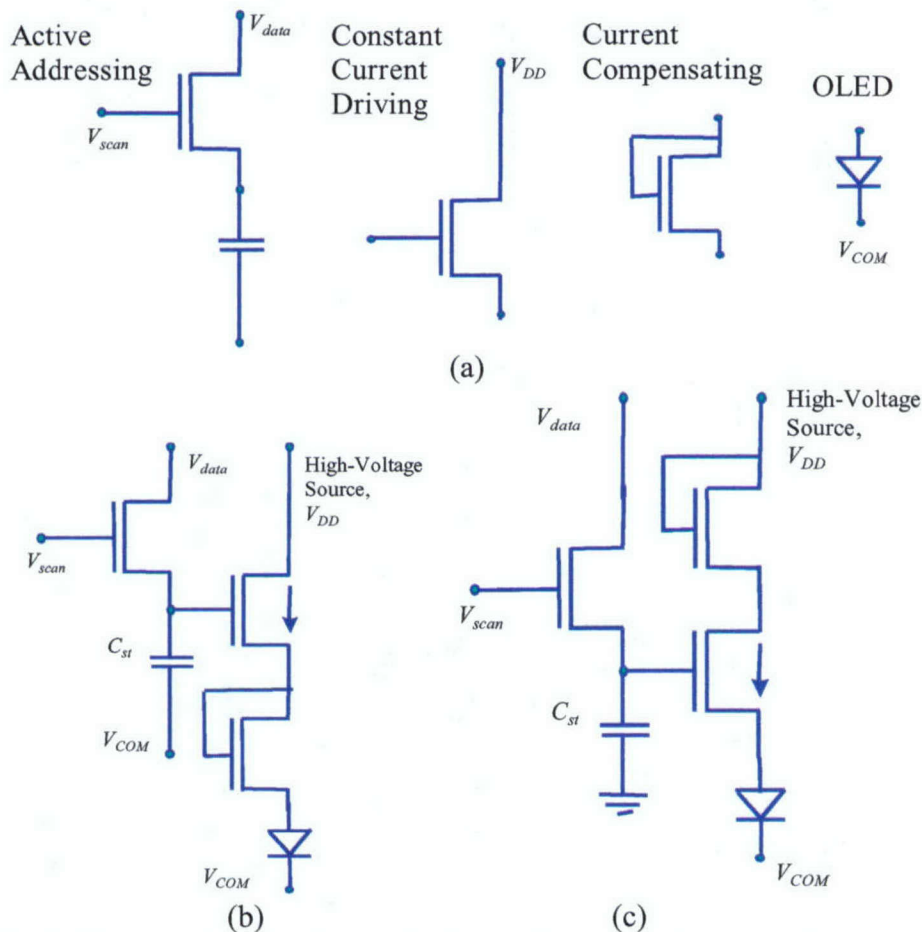


Figure 2. Equivalent pixel electrode circuit schematics for (a) circuit blocks and (b), (c) AM-OLED are shown.

One drawback of the pixel electrode circuit shown in the Figure 2 (b) is that the active resistor shares the voltage applied to the OLED and lowers the maximum voltage drop across the OLED. To overcome this limitation, the active load can be relocated to the topside of the constant

current driver TFT, Figure 2 (c). As shown in the Figures 2 (b) & (c), additional metal wiring for interconnection and a constant high voltage source is required to integrate component blocks proposed above.

#### 4.2 PIXEL ELECTRODE CIRCUIT DESIGN

The current source is a two terminal component whose current at any instant of time is independent of the voltage across their terminals [15]. Figure 3 (a) shows the TFT implementation of current source. The drain electrode is connected to the positive node at  $V_{DD}$ . The gate is set to a voltage ( $V_{GG}$ ) necessary to create a desired value of the output current. We should note that TFT operating in the non-saturation region is not desirable as current source, Figure 3 (b). In order for the current source to perform properly the voltage across the current source should be larger than  $V_{min}$ . The  $V_{min}$  is the minimum value of  $V_{DS}$  for which the TFT will remain in saturation region, e.g.

$$V_{OUT} \geq V_{GS} - V_T = V_{GG} - V_S - V_T = V_{min}$$

where  $V_{GS}$  is the drain-source voltage and  $V_T$  is the threshold voltage. Thus,  $V_{min}$  can be thought of as the minimum drain-source voltage for which the TFT remains in saturation. In this TFT operation region, the drain current can be written as:

$$i_{OUT} = \frac{\mu C_{OX} W}{2L} (V_{min})^2$$

where  $\mu$  is field effective mobility,  $C_{OX}$  is gate capacitance,  $W$  is channel width, and  $L$  is channel length. The  $V_{min}$  can be reduced by increasing the value of  $W/L$ . But at the same time the gate-source voltage must be adjusted for a given  $W/L$  ratio to produce the required output current:

$$V_{min} = \frac{1}{\sqrt{W/L}} \cdot \sqrt{\frac{2}{\mu \cdot C_{OX}}} \cdot (i_{OUT})^{1/2}$$

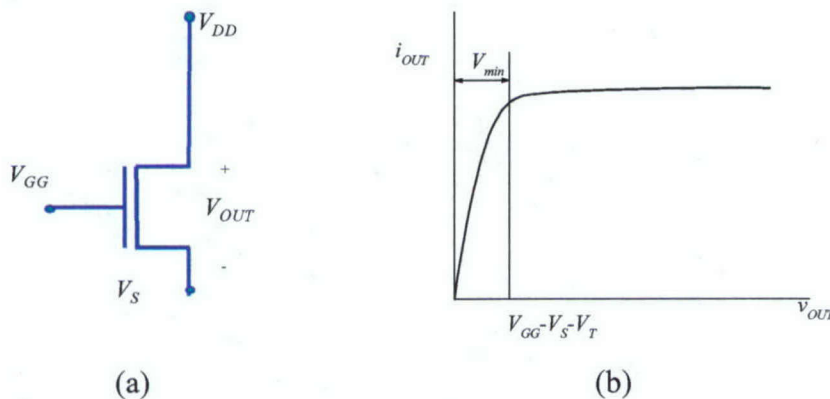


Figure 3. (a) Current source and (b) measured current-voltage characteristics of (a) are shown.

The active resistor was used in this circuit to compensate the change of the current flowing out of the current source. There are two factors that can change the output current of the current source. They are the threshold voltage change of the current source and the turn-on voltage shift of the OLED. The active resistor is achieved by simply connecting the gate to the drain electrode as shown in Figure 4 (a). Since the connection of the gate to the drain electrodes guarantees operation in the saturation region, the I-V characteristics, Figure 4 (b), can be described by:

$$i_D = \left( \frac{\mu C_{OX} W}{2L} \right) (V_{GS} - V_T)^2 = \beta' (V_{GS} - V_T)^2$$

or

$$V_{GS} = V_{DS} = V_T + \sqrt{i_D / \beta'}$$

where

$$\beta' = \frac{1}{2} \mu C_{OX} \frac{W}{L}$$

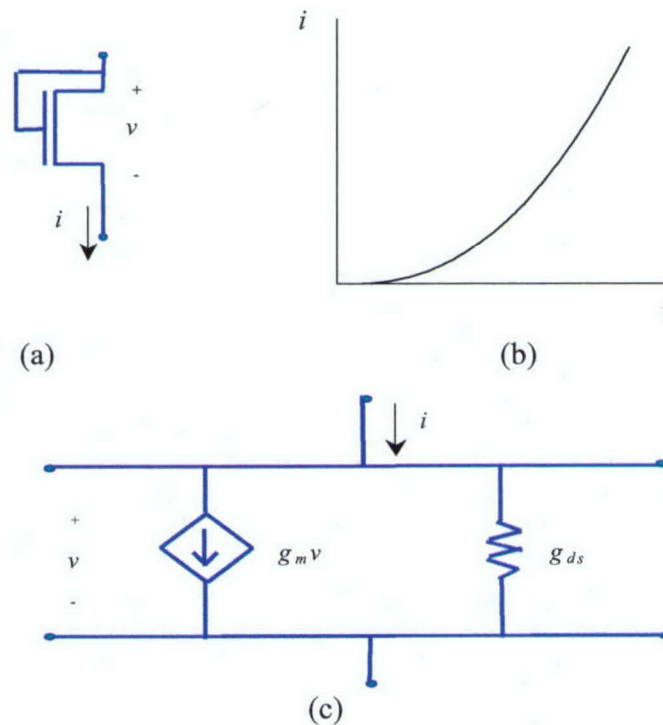


Figure 4. (a) Active resistor, (b) measured I-V characteristics, and (c) AC model are shown.

Connecting the gate to the drain electrode means that  $V_{DS}$  controls  $i_D$  and, therefore, the channel transconductance becomes a channel conductance, Figure 4 (c). The output resistance of this active resistor is given by:

$$r_{out} = \frac{1}{g_m + g_{ds}} \cong \frac{1}{g_m} \propto \frac{1}{\sqrt{|I_{DS}|}}$$

$$g_m = \sqrt{(1/\beta')I_D(1+\lambda V_{DS})} \cong \sqrt{|I_{DS}|/\beta'}$$

$$g_{ds} = g_o = \frac{I_D \lambda}{1 + \lambda V_{DS}} \cong I_D \lambda$$

where  $\lambda$  is channel-length modulation parameter. Clearly, the output resistance of the active resistor is inversely related to the current. The rate at which the current will change can be increased by increasing the W/L ratio.

#### 4.3 PIXEL ELECTRODE CIRCUIT DRIVING SCHEME

The pixel electrode circuit operation of 3-TFT AM-OLED can be described as follows. During the scan time, the gate scan voltage ( $V_{scan}$ ) pulses to a high level, Figure 5 (b). While  $V_{scan}$  is high, an image data ( $V_{data}$ ) is fed to the gate electrode of the constant current driving TFT controlling the amount of the drain current (driving current) of the driving TFT. The drain electrode of the driving TFT is connected to a high-voltage source through the active resistor. At the same time,  $V_{data}$  is stored in the storage capacitor ( $C_{st}$ ). For a given frame time depending on the refresh rate of the AM-OLED design, the gate voltage of the constant current driving TFT remains at the same level even after  $V_{scan}$  drops low, since  $C_{st}$  keeps the image data ( $V_{data}$ ).

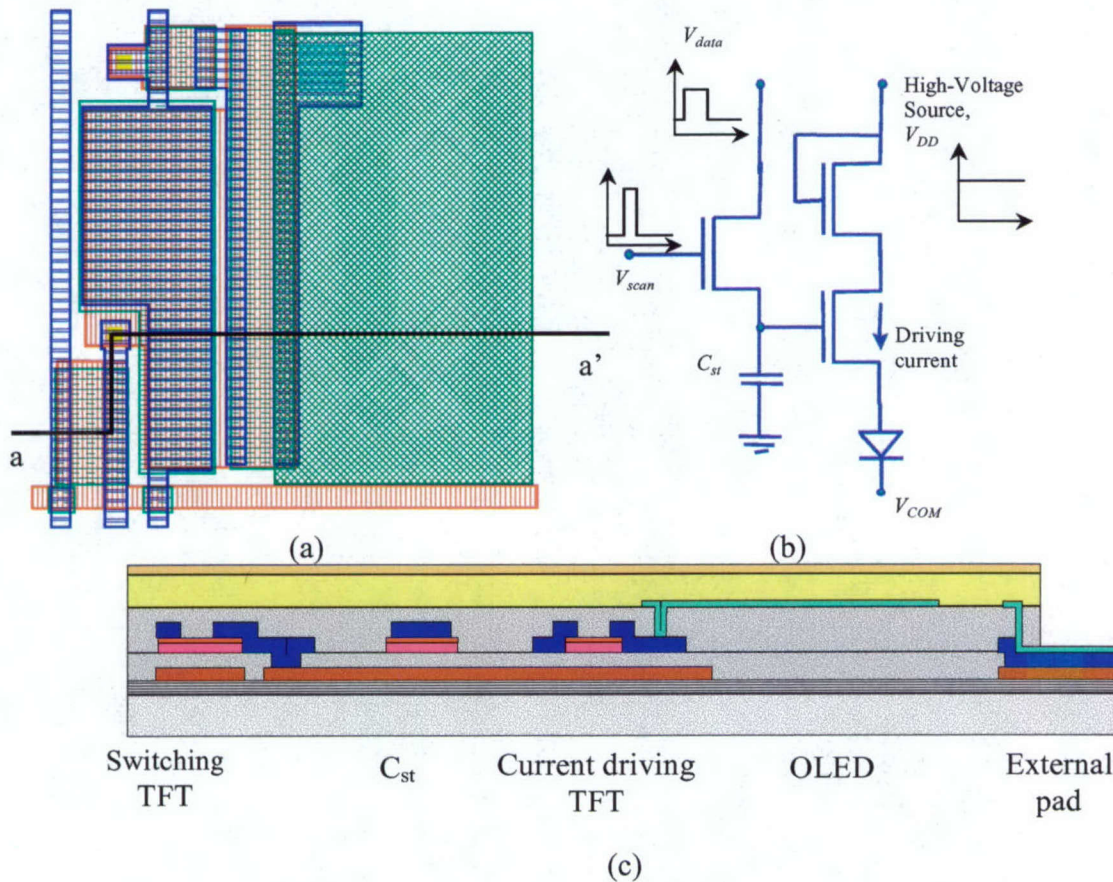


Figure 5. (a) Top view of the mask layout, (b) schematic, and (c) cross-section (a – a') of the AM-OLED pixel electrode circuit are shown.

Active resistor is a TFT with gate and drain electrodes connected together operating in saturation mode only. The operating current determines the voltage drop across the active resistor. For any reason, e.g. when the threshold voltage of the constant current driver increases or the turn-on voltage of the OLED increases, if the current flowing through the active resistor decreases, the voltage drop across the active resistor decreases. That will allow for a high current to flow back through the OLED pixel, compensating for the parameter changes in both the constant current driver and the OLED. Figure 5 shows the layout, the pixel electrode circuit diagram, and the cross-section of our AM-OLED.

#### 4.4 PIXEL ELECTRODE CIRCUIT SIMULATION

The pixel electrode circuit performance of the AM-OLED was simulated using the Cadence circuit simulator, Spectra. The a-Si:H TFT model was previously developed within our group [16]. The OLED was fabricated using spin-coated organic materials [4]. The measured OLED characteristic is shown in the Figure 6. The OLED light emission started at about 12 V. The output current ranged from 0 to 3 mA for the applied voltage range from 12 to 30 V, Figure 6. The current-voltage characteristics show a linear relationship in the device operating range.

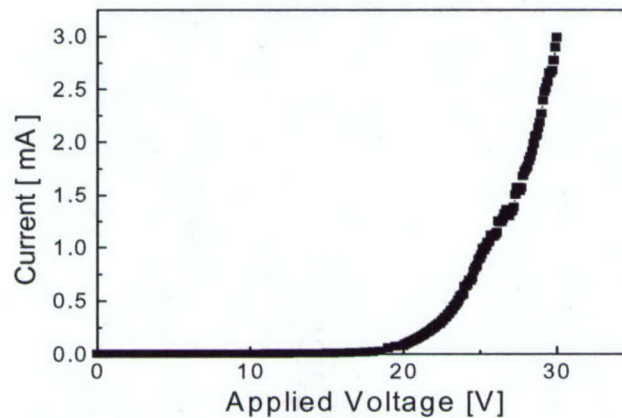


Figure 6. Measured current-voltage characteristics of spin-coated OLED fabricated in our laboratory is shown.

For the OLED model, a semiconductor diode model was used and fitted to the measured data, Figure 7. Using the model parameters and pixel electrode circuit shown in Table 2 and Figure 5 (b), respectively, the 100 x 100 active-matrix arrays for AM-OLED with 200 dpi resolution (127  $\mu\text{m}$  x 127  $\mu\text{m}$  pixel size) was designed and simulated for three different driving voltages, 20, 30 and 40 V, Figure 8. In each case, the data and the scan voltages were the same as the driving voltages,  $V_{\text{drv}}$ . The transient pixel electrode circuit simulation results are shown for 30 msec case. The ON- and OFF-states are shown in Figures 8 (a) and (b). The detail views are also shown for the transition periods between ON- and OFF-states in the Figures 8 (a') and (b') for two different driving voltages. The storage capacitance was optimized during the AM-OLED simulation. The optimum value was chosen to be large enough for good image retention and to fit into the pixel area (e.g. pixel electrode aperture ratio was optimized).

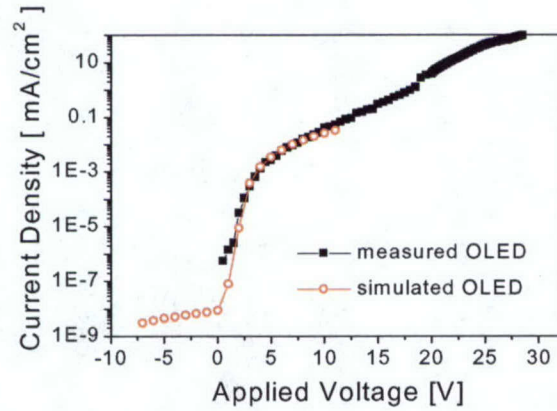
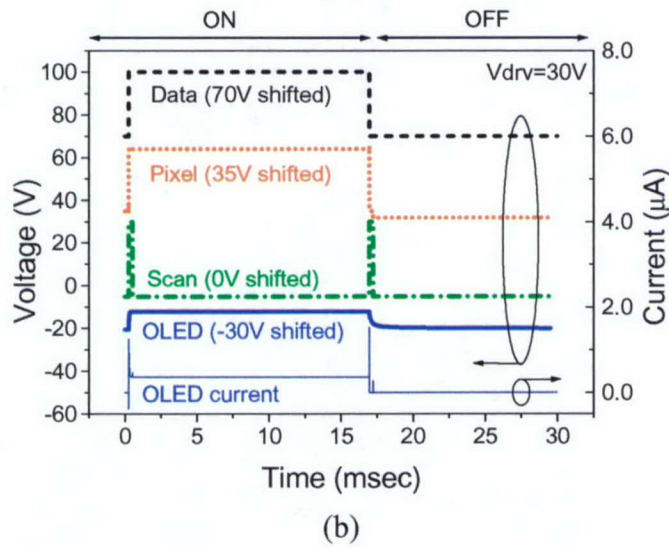
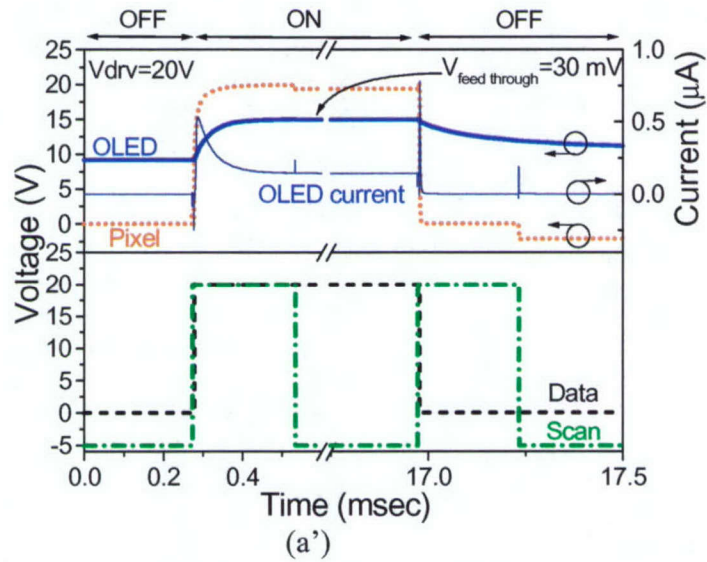
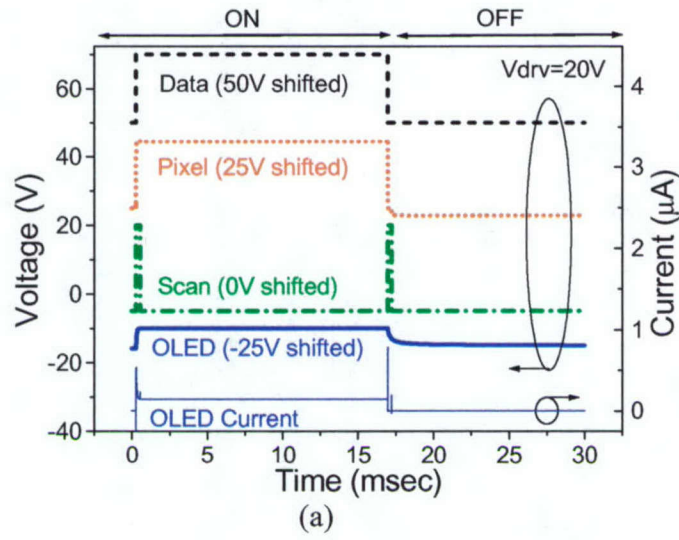


Figure 7. The measured OLED characteristic and curve fitting with a two terminal semiconductor diode model used for pixel electrode circuit simulation are shown.

Table 2. The AM-OLED pixel design parameters.

DESIGN PARAMETERS	VALUE
Gate-bus width, $W_{gate}$	15 $\mu\text{m}$
Gate-bus thickness, $t_{gate}$	0.2 $\mu\text{m}$
Data-bus width, $W_{data}$	8 $\mu\text{m}$
Data-bus thickness, $t_{data}$	0.3 $\mu\text{m}$
Current driving TFT channel width, $W_{drv}$	110 $\mu\text{m}$
Current driving TFT channel length, $L_{drv}$	10 $\mu\text{m}$
Active resistor channel width, $W_{ar}$	15 $\mu\text{m}$
Active resistor channel length, $L_{ar}$	10 $\mu\text{m}$
Switching TFT channel width, $W_{sw}$	30 $\mu\text{m}$
Switching TFT channel length, $L_{sw}$	10 $\mu\text{m}$
Storage capacitor, $C_{st}$	0.3 pF

With a storage capacitance of 0.3 pF, the switching between the ON- and OFF-states was completed within the scan time. In addition, the image data stored in the storage capacitor was retained without any loss during the retention period for AM-OLED frame time (60 Hz). In both the AM-LCD and the AM-OLED pixels, the feed-through voltage drops occur while the  $V_{scan}$  signal drop. Feed-through voltage is an abrupt voltage change induced by a capacitive coupling of the gate signal through the gate-source capacitance. Typically, the AM-LCD pixel electrode circuit has a feed-through voltage of about 1 to 2 V at the source electrode of the switching TFT [17]. On the other hand, the feed-through voltage of our AM-OLED pixel is only of a few tenth of mV. This was achieved by using the cascaded TFT connection of the switching TFT and the constant current driving TFT. This low feed-through voltage will enhance the gray level controllability of the AM-OLED. Another advantage of the gray level control in AM-OLED over AM-LCD is the absence of the asymmetrical feed-through voltage effect associated with the dual data voltage levels ( $V_{d+}$  and  $V_{d-}$ ).



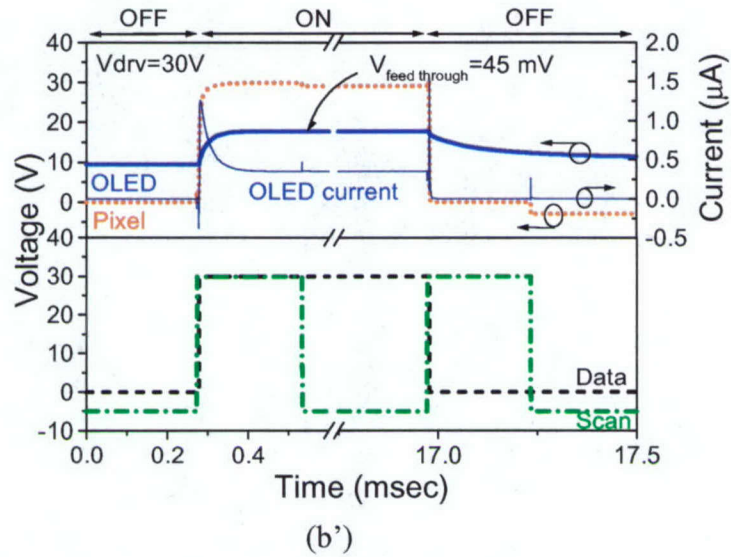


Figure 8. (a) and (b) Simulation examples and (a') and (b') the details of the AM-OLED operation for driving voltages of 20 and 30 V are given.

To simulate the current-compensation method developed during this study, three different device parameter shifts have been considered, Figure 9. The driving current was maintained constant while there was a threshold voltage shift introduced on the constant current driving TFT. For the threshold voltage shift of the active resistor and the turn-on voltage shift of the OLED, the driving current reduced down to 60 % of its initial value. It was difficult to compensate for these shifts. However, this current-compensation method can be improved by adapting common gate driving configuration for the constant current driving TFT. This type of configuration will require OLED with the ITO-on-top structure. The extensive pixel electrode circuit simulation and analysis results indicate that a continuous pixel electrode excitation can be achieved with these circuits, and a pixel electrode driving output current level up to  $1.4\ \mu\text{A}$  can be reached with a-Si:H TFT technology.

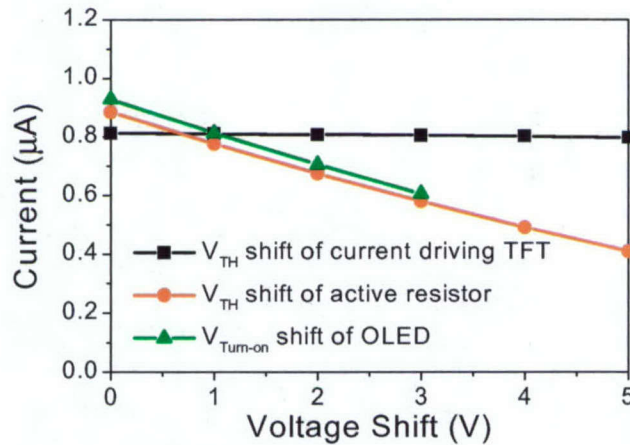


Figure 9. Variation of the output current with  $V_{TH}$  shift of current driving TFT and active resistor, and with  $V_{Turn\ on}$  shift of OLED are shown.

#### 4.5 AM-OLED OPERATION

The 3 – a-Si:H TFT pixel electrode circuit developed during this project is shown in Figure 10 (a) [18]. Each pixel circuit features 3 TFTs. In this schematic diagram,  $C_{ST}$  is storage capacitor, T1 is switching TFT, T2 is active resistor, and T3 is large-sized high-capacity constant current driving TFT. The image data signals are digitized to data voltage ( $V_{data}$ , 0 to 15 V in this example). The pixel electrode circuit performance of our AM-OLED was simulated using the circuit simulator, HSPICE. Using the OLED and a-Si:H TFT models developed during this research, an active-matrix array of 640 x 480 pixels (VGA) for AM-OLED with 200 dpi resolution ( $127 \mu\text{m} \times 127 \mu\text{m}$  pixel size) was designed and simulated for data voltages ( $V_{data}$ ) ranging from 0 to 15 V. An example of the transient pixel electrode circuit simulation is shown in Figure 10 (b), where we plot two image data voltages of 15 and 0 V for maximum and minimum output current cases, respectively. The proper sizing of each TFTs (W/L) was determined through the pixel electrode circuit simulation.

While  $V_{select}$  stays high, the switching TFT turns on, and then the data voltage,  $V_{data}$ , is transferred and stored in the storage capacitor providing the turn-on signal to the gate electrode of the driver TFT. This selecting operation of each pixel occurs during a very short period of time, called scan period. Usually this scan period is defined by the number of rows of the display. For instance, 21.7 and 16.3  $\mu\text{sec}$  are the scan periods for SVGA and XGA displays operated at 60 Hz, respectively. In order to fully charge the storage capacitor up to the data voltage level, the speed of the switching TFT is important. Depending on the data voltage level which is now applied to gate electrode of the driver TFT, the driver TFT provides the corresponding current (output current,  $I_{out}$ ) to the OLED. For this current level, the OLED will emit light corresponding to certain brightness level. Hence, the maximum brightness of the OLED depends on the current capacity of the driver TFT and the external luminance efficiency of the OLED.

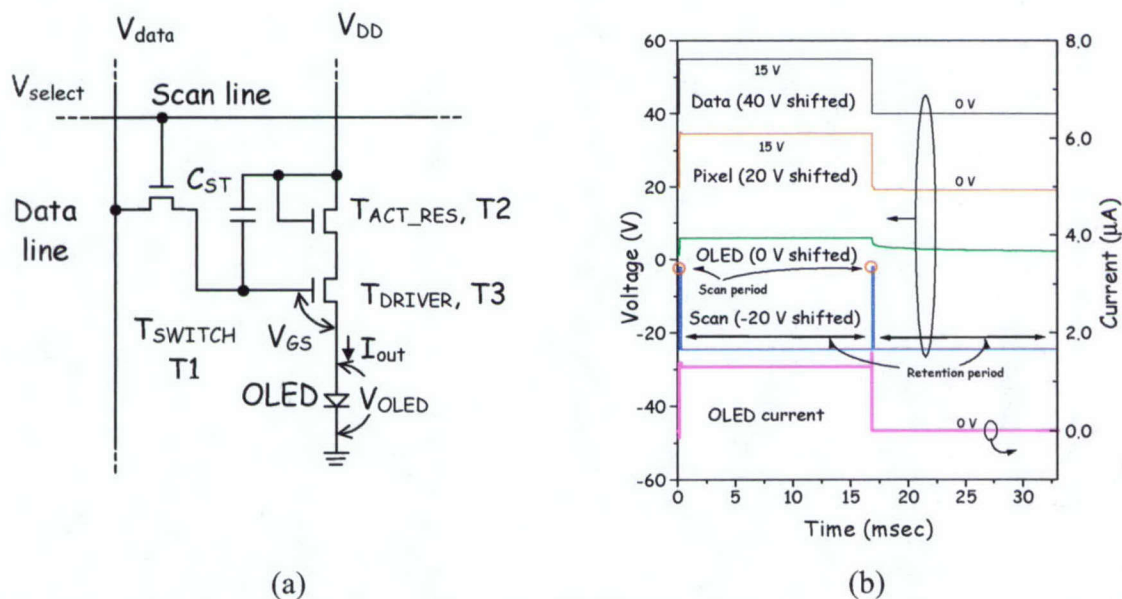


Figure 10. A (a) schematic diagram of the AM-OLED pixel electrode circuit and a (b) simulation example of the AM-OLED operation for data voltages of 15 V are shown.

After the scan period, a long retention period of about 17 msec occurs. During the retention period,  $V_{\text{select}}$  stays low and the switching TFT turns off disconnecting the data line from the driver TFT. Nonetheless, the output current level needs to be maintained at the same level for keeping the OLED brightness level unchanged. To accomplish this, the charge in the storage capacitor needs to be maintained for the entire retention period since  $C_{\text{ST}}$  keeps the image data ( $V_{\text{data}}$ ). A very low OFF-current (negligible to the ON-current) of the switching TFT is a must. In other words, a high ON / OFF current ratio of the switching TFT is required. During the repetition of scan and retention periods, the same or new image will be refreshed or shown.

As indicated above the current compensation circuit is represented by an active resistor (T2) TFT operating only in saturation mode. The voltage drop across the active resistor is determined by the output current level which flows through OLED since both the active resistor and OLED are on the same current path. Over time, the TFT threshold voltage of the constant current driver or the OLED turn-on voltage increases due to the device characteristic shifts caused during the display operation resulting in the output current decrease. When the output current decreases, the voltage drop decreases as well, allowing a higher drain – source voltage of the driver TFT. That will allow for a high current to flow back through the OLED pixel, compensating for the device parameter changes in both the constant current driver TFT and the OLED. That changes the operating condition of the driver TFT. This type of current compensation can only provide a limited negative feedback for the pixel electrode circuits. According to our circuit simulation results, however, the degree of compensation can be adequate for the pixel circuit with well optimized design.

#### *4.6 AM-OLED PIXEL ELECTRODE CIRCUITS FABRICATION*

Based on our design, active-matrix array for 3 – a-Si:H TFT AM-OLED has been successfully fabricated in our laboratory. Figure 11 shows the top views of the quarter-size active-matrix arrays and the AM-OLED panel. A continuous pixel electrode excitation was achieved with these pixel circuits, and the output driving current level was reached up to 1.3  $\mu\text{A}$  with this a-Si:H TFT technology. The conventional back-channel etched (BCE) TFTs technologies were used with  $n^+$  a-Si:H/a-Si:H/a-SiN<sub>x</sub>:H layers deposited by plasma-enhanced chemical vapor deposition (PECVD) technique at substrate temperature of 300 °C [19].

In this 200 dpi AM-OLED the active-resistor had a channel width of 15  $\mu\text{m}$ , and the driving and switching TFTs had channel widths of 105 and 30  $\mu\text{m}$ , respectively, with the same channel length of 10  $\mu\text{m}$ . The storage capacitance was 0.4 pF. The cross-section view of the AM-OLED backplane is also shown in Figure 11; the inset shows a blow-up of single pixel electrode circuit. The light is emitted from the back side of the display through the glass substrate. The storage capacitor is 0.4 pF, and the pixel aperture ratio is 45 % for this pixel design. With a storage capacitance of 0.4 pF, the switching between the ON- and OFF- pixel electrode states was completed within the scan time. In addition, the image data stored in the storage capacitor was retained without any loss during the retention period for AM-OLED frame time (60 Hz). In the present design, OLED area is 7200  $\mu\text{m}^2$ .



arrays was accomplished at the Solid-State Electronics Laboratory of The University of Michigan.

The active-island was defined with the RIE etching using  $\text{CCl}_2\text{F}_2$  and  $\text{O}_2$  gas mixture (mask #2). Opening of the gate contact via was done with one step wet etching through a-SiN<sub>x</sub>:H layer in buffered hydro-fluoric acid (BHF) (mask #3). The a-SiN<sub>x</sub>:H layer was etched at fast rate without any residue formation. A Mo source/drain metal layer was deposited by DC magnetron sputtering at room temperature. Before the source/drain electrodes metallization, any native oxide present on the surface of n<sup>+</sup> a-Si:H layer was removed by a quick dip in commercial BHF solution.

The source/drain electrodes were defined with wet etching solution of a mixture of phosphoric acid, nitric acid, acetic acid, and DI water (mask #4). The channel etch-back of the n<sup>+</sup> a-Si:H followed the source/drain patterning without additional photo mask using RIE method. For this RIE step the same plasma chemistry was used as for active-island patterning but with a lower power density for precise control of the etch depth. This depth needs to be optimized for the control of the a-Si:H TFT OFF-current level.

Then, the source/drain electrodes were planarized with BCB using spin-coater. The spun film was cured in a furnace at 250 °C in nitrogen ambient. Opening of the top-via was done with the RIE etching using  $\text{CF}_4$  and  $\text{O}_2$  gas mixture (mask #5). An ITO (OLED anode) metal layer was deposited by DC magnetron sputtering at room temperature, and then cured in a furnace at 250 °C in nitrogen ambient. The anode electrode was defined with wet etching in a wet etching solution of a mixture of HCl, nitric acid, and DI water (mask #6). The typical thickness of each layer in this case was 3000 Å for Cr, 3000 Å for a-SiN<sub>x</sub>:H, 2500 Å for a-Si:H, 300 Å for n<sup>+</sup> a-Si:H, 1000 Å for Mo, 3000 Å for BCB, and 1000 Å for ITO.

Once the active-matrix array was fabricated, a hole injection layer (HIL) and a light emissive layer (LEL) was spin-coated. Poly(3,4-ethylene dioxythiophene) (PEDOT) doped with poly(styrenesulfonate) (PSS) and green light-emitting poly (fluorene) copolymer were used for HIL and LEL materials, respectively. Finally, a calcium/aluminum bi-layer cathode was thermally evaporated through a shadow mask without breaking vacuum under  $\sim 10^{-6}$ Torr.

The driver TFT is used to provide continuous current ( $I_{\text{out}}$ ) to the OLED. The  $I_{\text{out}}$  at anode (ITO - positively biased) electrode will establish an electrical potential difference between ITO and cathode electrode (Ca/Al - negatively biased). Established electrical field will induce electron injection into and extraction from cathode and anode into LUMO and HOMO levels of the polymer, respectively. The process of removal of a negative charge (electron) from HOMO leaves a positive charge (or hole) in the band. This process can be referred to as a "hole injection" into polymer HOMO levels. Under the influence of an electrical field, the oppositely charged radicals (anions and cations) will drift toward each other from polymer chain to polymer chain. Finally, when they combine on a single conjugated segment, singlet and triplet excitonic states are formed, of which the singlets can radiatively decay with the emission of visible green light.

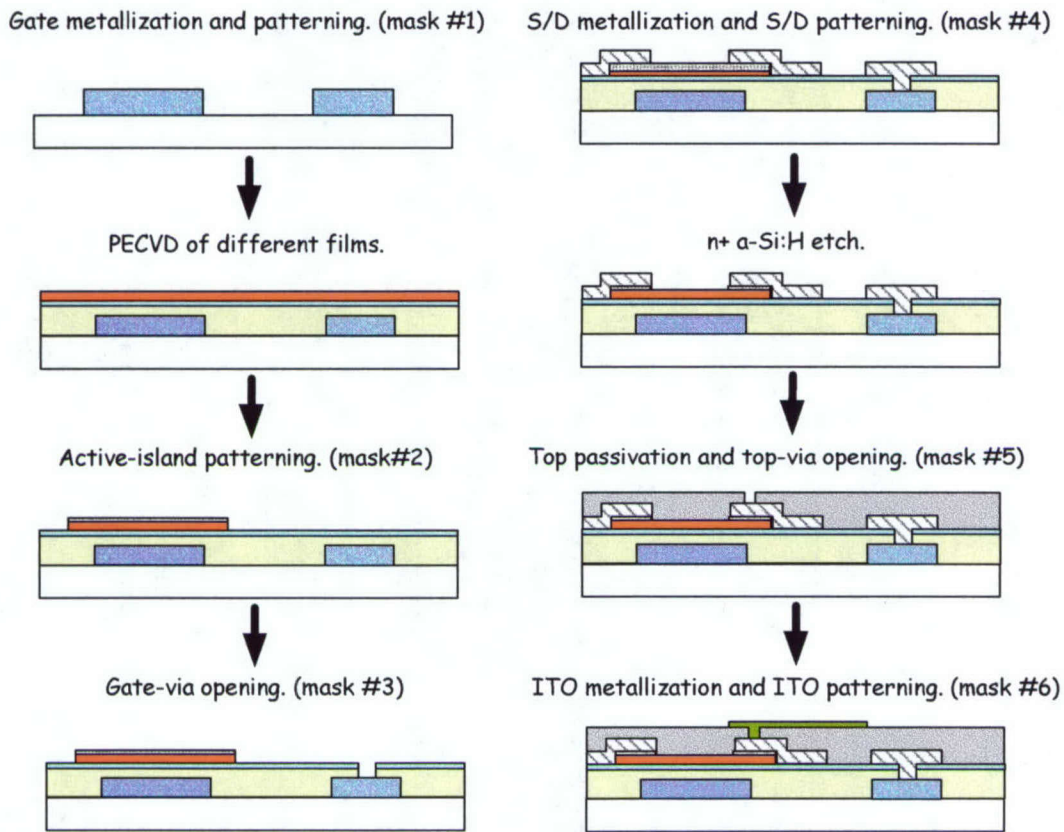


Figure 12. An example of the process flow of a-Si:H TFT-based pixel electrode circuit is shown.

#### 4.7 AM-OLED PIXEL ELECTRODE CIRCUIT PERFORMANCE

The output current of our AM-OLED pixel was measured with  $V_{DD} = 20\text{ V}$  and  $V_{scan} = 20\text{ V}$ , Figure 13. The maximum current density of  $21\text{ mA} / \text{cm}^2$  was achieved for the pixel electrode

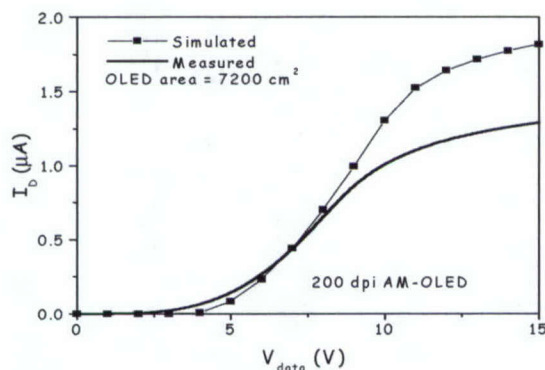


Figure 13. The measured and simulated AM-OLED output current versus input data voltage characteristics are shown.

aperture ratio of 45 % used in our design. The current density level can be adjusted from 5 to  $100\text{ mA} / \text{cm}^2$  by increasing the driver TFT size. At the same time the pixel electrode area will

be reduced. For  $I_{out} = 100 \text{ mA} / \text{cm}^2$ , the pixel aperture ratio would be reduced to about 25 % for display with resolution ranging from 200 to 500 dpi. The deviation between the simulated and measured results is mainly due to un-optimized active-matrix fabrication process conditions as mentioned above.

The calculated OLED brightness values for the output current level of  $21 \text{ mA} / \text{cm}^2$  are 4500, 210, and  $190 \text{ cd} / \text{m}^2$  for green (540 nm), blue (480 nm), and red (650 nm). In this case, OLED external quantum efficiency is assumed to be 5, 1.5, and 2 %, respectively, Figure 14. If the  $I_{out}$  id increased up to  $100 \text{ mA} / \text{cm}^2$ , the maximum OLED brightness levels that are possible with our pixel electrode circuits are 24000, 1200, and  $900 \text{ cd} / \text{m}^2$  for green, blue, and red, respectively.

The luminance shown in Figure 14 was calculated as follows:

$$L = 683 \times E(\omega) \cdot \eta_{ex} \cdot \frac{hc}{\pi\omega} \cdot \frac{J}{e}$$

where E is the normalized luminous efficiency (0.107, 0.954, and 0.139 for red, green, and blue, respectively, from photopic eye response curve),  $\omega$  is the wave length,  $\eta_{ex}$  is the device external quantum efficiency, h is the Planck constant, c is the velocity of light, e is the electronic charge, and J is the applied current density. It should be noticed that the OLED brightness levels for different colors will increase with the increase of the external quantum efficiencies and decreasing pixel electrode area.

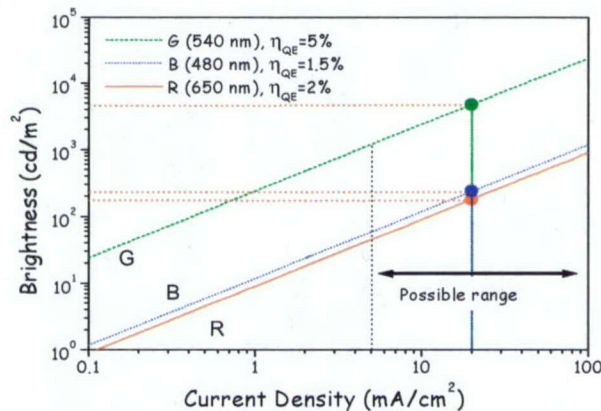


Figure 14. The maximum OP-LED brightness of each pixel for RGB color scales.

#### 4.8 AM-OLED OPTO-ELECTRONIC PROPERTIES

The test display unit fabricated in our laboratory during this project was operated to illuminate the whole display without packaging and driver electronics, Figure 15. The display size is 0.7 inch diagonal with 100 by 100 pixels. Very uniform light intensity among pixels across the display was observed under the microscope, Figure 15 (inset). However, there are a few line defects of the  $V_{DD}$  bus or data signal bus lines and some pixel defects with bright spots.

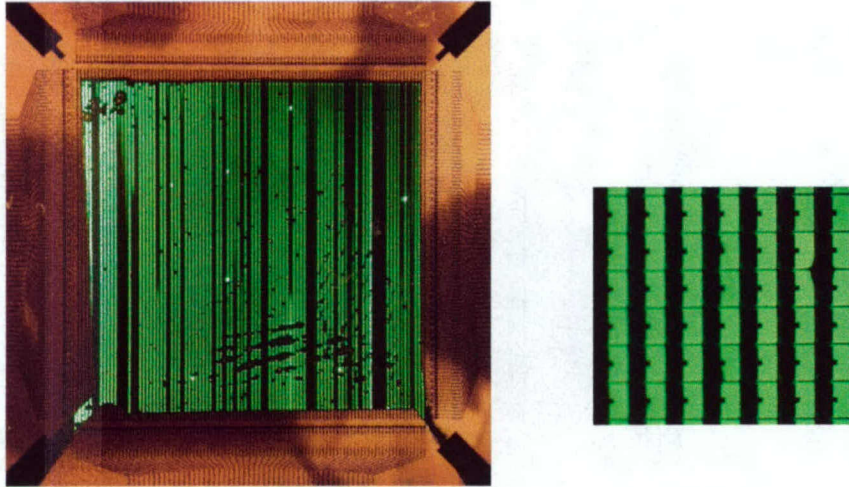


Figure 15. Top and blow-up views of illuminated AM-OLED are shown. The bright area on the left is glare from the light. The OLED size was about  $120\ \mu\text{m} \times 62.5\ \mu\text{m}$  for pixel size of  $127\ \mu\text{m} \times 127\ \mu\text{m}$ . The fill factor was about 45 %.

The opto-electrical characteristics of the AM-OLED have been measured using an integrating sphere and a calibrated photo-detector connected to a radiometer to measure the total luminous flux. To light up the display we continuously applied a DC signal (30 V) to all the scan lines and  $V_{\text{DATA}}$  signal was varied from 0 to 30 V for different grey scales. All the measurements have been performed in the air at room temperature.

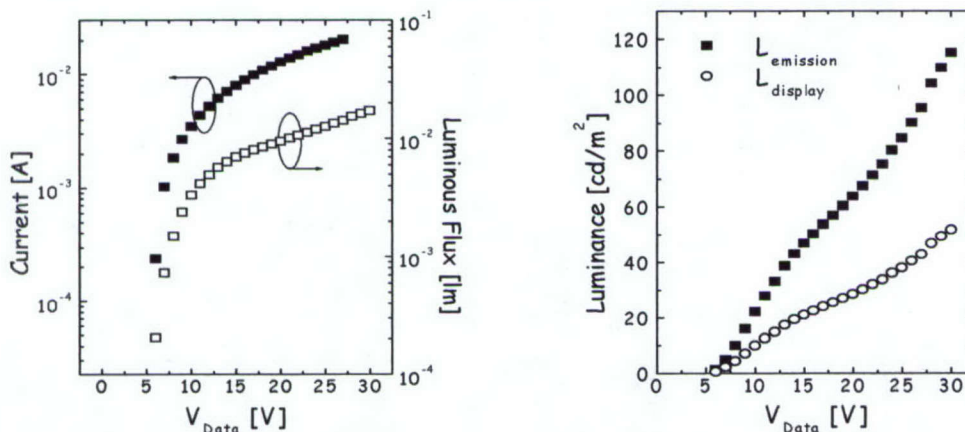


Figure 16. (a) Measured current and luminous flux and (b) luminance of our AM-OLED.

Figure 16 (a) shows the current and luminous flux versus data voltage characteristics. The initial light emission is observed when  $V_{\text{DATA}}$  is about 4~5 V. We can consider this data voltage as a turn-on data voltage that is closely related to the green OLED turn-on voltage and the  $V_{\text{DS}}$  of the switching TFT (T1) and the  $V_{\text{GS}}$  of the driving TFT (T3) during selection time. We obtained up to  $2 \times 10^{-2}$  lumen at  $V_{\text{DATA}} = 30$  V. The display luminance was estimated from the optical flux, assuming that the AM-OLED has Lambertian emission (it was checked experimentally that OLED luminance was constant over the whole considered angular domain). The total display

area of  $1.27\text{cm} \times 1.27\text{cm} = 1.62 \times 10^{-4} \text{m}^2$  results in the display luminance:

$$L_{display} = \Phi / (\pi \times 1.6 \times 10^{-4})$$

However, we also need to consider the actual light-emitting area to calculate the effective luminance of the light-emitting areas ( $L_{emission}$ ), which can be expressed as  $A_{emission} = (\text{total \# of pixels}) \times (\text{yield of emitting pixels}) \times (\text{OLED area in each pixel})$ . For our 200 dpi AM-OLED, this area is  $A_{emission} = 4.74 \times 10^{-5} \text{m}^2$ , where the yield of emitting pixels ( $\sim 65\%$ ) was estimated from Figure 15.

Figure 16 (b) shows the evolution of the luminances with the data voltage. The estimated luminance values ( $L_{display}$  and  $L_{emission}$ ) at maximum luminous flux are about 50 and 120  $\text{cd}/\text{m}^2$ , respectively. These values can be increased through optimization of the AM-OLED.

1. D.R. Baigent, N.C. Greenham, J. Gruener, R.N. Marks, R.H. Friend, S.C. Moratti and A.B. Holmes, "Light-Emitting Diodes Fabricated with Conjugated Polymers – Recent Progress," *Synthetic Metals*, **67**, 3 (1994).
2. J. Kido, M. Kimura, and K. Nagai, "Multilayer White Light-Emitting Organic Electroluminescent Device," *Science*. **267**, 1332 (1995).
3. C. Hosokawa, M. Matsuura, M. Eida, K. Fukuoka, H. Tokailin, and T. Kusumoto, "Full-Color Organic EL Display," *J. of SID* **6**, 257 (1998).
4. Y. He, S. Gong, R. Hattori, and J. Kanicki, "High Performance Organic Polymer Light-Emitting Heterostructure Devices," *Appl. Phys. Lett.*, **74** (1999).
5. T. Shimoda, H. Ohshima, S. Miyashita, M. Kimura, T. Ozawa, I. Yudasaka, S. Kanbe, H. Kobayashi, R.H. Friend, J.H. Burroughes, and C.R. Towns, "High Resolution Light Emitting Polymer Display Driven by Low Temperature Polysilicon Thin Film Transistor with Integrated Driver," *Proceedings of Asia Display '98*, p. 217 (1998).
6. M. Stewart, R.S. Howell, L. Pires, M.K. Hatalis, W. Howard, and O. Prache, "Polysilicon VGA Active matrix OLED Displays – Technology and Performance," *Proceedings of IEDM*, p. 871 (1998).
7. R.M.A. Dawson, Z. Shen, D.A. Furst, S. Conner, J. Hsu, M. G. Kane, R.G. Stewart, A. Ipri, C.N. King, P.J. Green, R.T. Flegal, S. Pearson, W.A. Barrow, E. Dickley, K. Ping, C.W. Tang, S.V. Slyke, F. Chen, J. Shi, J. C. Sturm, and M.H. Lu, "Design of an Improved Pixel for a Polysilicon Active-Matrix Organic LED Display," *SID 98 Digest*, 11 (1998).
8. J.-H. Kim, C.-Y. Chen, B.-H. Min, and J. Kanicki, "Aluminum Gate Metallization for High-Performance a-Si:H TFTs Fabricated from High-Deposition Rate PECVD Materials," *Proceedings of the International Display Research Conference*, p. 49 (1997).
9. J.-H. Kim, E.S. Moyer, K. Chung, and J. Kanicki "Gate Planarized a-Si:H TFTs with the Silicon-based Flowable Oxide," *Proceedings of the International Display Research Conference*, p. 443 (2000).
10. Y. He, R. Hattori, and J. Kanicki, "Four-Thin Film Transistors Pixel Electrode Circuits for Active-Matrix Organic Light-Emitting Displays," *Japan Journal of Applied Physics*, **40**,1 (2001).
11. Y. He, R. Hattori, and J. Kanicki, "Current-Source a-Si:H Thin-Film Transistors Circuit for Active-Matrix Organic Light-Emitting Displays," *IEEE EDL*, **21**, 590 (2000).
12. Y. He, R. Hattori, and J. Kanicki, "Electrical Reliability of Two- and Four-a-Si:H TFT Pixel Electrode Circuits for Active-Matrix OLEDs," *Proceedings of International Display Research Conference*, p. 354 (2000).
13. K. Doi, M.L. Giger, R.M. Nishikawa, and R.A. Schmidt, editors, "Technical Aspects of Digital Mammography," *Digital Mammography, Elsevier Science*, p. 33-41 (1996).
14. L.L. Fajardo and M.B. Williams, "The Clinical Potential of Digital Mammography," *Digital Mammography, Elsevier Science*, p. 43-52 (1996).
15. P.E. Allen and D.R. Holberg, *CMOS Analog Circuit Design*, p. 219, Saunders College Publishing (1987).

16. . C.-Y. Chen and J. Kanicki, "High-Performance a-Si:H TFT for Large-Area AMLCDs," *Proc. of ESSDERC '96*, p. 1023 (1996).
17. Ohta, M. Tsumura, J. Ohida, J. Ohwada, and K. Suzuki, "Active Matrix Network Simulation Considering Nonlinear C-V Characteristics of TFT's Intrinsic Capacitances," *Japan Display*, p. 431 (1992).
18. J.-H. Kim and J. Kanicki, "Advanced Amorphous Silicon Thin Film Transistor Active-Matrix Organic Light-Emitting Displays Design for Medical Imaging," *Proc. of SPIE*, **4319**, 306 (2001).
19. J.-H. Kim, J. Kanicki and W. den Boer, "Aluminum Gate Metallization for AMLCDs," *Mat. Res. Soc. Symp. Proc.*, **471**, 111 (1997).

## 5. KEY RESEARCH ACCOMPLISHMENTS

In this project, we have achieved the following accomplishments:

- The AM-OLED pixel electrode circuits have been developed with four components: switching TFT, constant-current driving TFT, active resistor, and OLED. In our work all TFTs are based on the a-Si:H technologies. The maximum output pixel electrode driving current was 1.4  $\mu\text{A}$ , and the AM-OLED brightness of  $\sim 88$ ,  $\sim 960$ , and  $\sim 160$   $\text{cd}/\text{m}^2$  can be achieved for red (650 nm), green (540 nm), and blue (480 nm) light emission, respectively. We have clearly shown that a-Si:H TFT technology in combination with the OLED can be used to design AM-OLED for medical imaging applications.
- We have demonstrated that it is possible to develop a high-resolution AM-OP-LED based on a-Si:H TFT technology. The pixel electrode circuits simulation and experimental results indicate that a continuous pixel electrode excitation can be achieved with these pixel circuits, and a pixel electrode driving output current level up to 1.3  $\mu\text{A}$  can be reached with the a-Si:H TFT technology. We also think that the output current density level can be increased up to 100  $\mu\text{A} / \text{cm}^2$  for optimized pixel electrode circuits.
- We fabricated a small size engineering 200 dpi AM-OLED based on a 3- a-Si:H TFT pixel electrode circuit. We have shown that a-Si:H TFTs can provide sufficient out current for AM-OLED. The brightness of our display increases almost linearly up to 120  $\text{cd}/\text{m}^2$  with  $V_{\text{DATA}}$  ranging from 0 V to 30 V.

These accomplishments represent the completion of Task 1 and 4 described in the proposal.

## 6. REPORTABLE OUTCOMES RESEARCH

### PRESENTATIONS

### PRODUCTS

3-a-Si TFT AM-PLLED working prototype was fabricated during this project.